Characterization of Alkali-Doped Ni/SiO_2 Catalysts

A. Díaz,[†] D. R. Acosta,[‡] J. A. Odriozola,[§] and M. Montes*

Grupo de Ingeniería Química, Departamento de Química Aplicada, Facultad de Ciencias Químicas de San Sebastián, Universidad del País Vasco, Apdo. 1072, 28080 San Sebatián, Spain

Received: October 14, 1996; In Final Form: January 1, 1997[⊗]

The effects of the alkali doping on the reducibility and morphological properties together with distribution and crystallography of phases of a Ni/SiO_2 catalyst have been investigated by N_2 adsorption measurements, diffuse reflectance IR Fourier transform spectroscopy (DRIFTS), CO adsorption, DRIFTS determinations, temperature-programmed reduction (TPR), X-ray diffraction line broadening (XRDLB), H_2 chemisorption, and TEM observations. Alkaline dopants produce an increase in the weakly adsorbed fraction of hydrogen and important changes in the adsorption modes of CO. Lithium and potassium modify the distribution of Ni across the support, inducing sintering phenomena, while sodium keeps nickel particle dispersion.

Introduction

The use of alkali metals as catalytic promoters or modifiers of the activity of heterogeneous catalyst, or to improve their lifetime, has been a part of catalytic technology for many years.[1−4] However, the role played by alkali metals is not unequivocal, depending on the type of solid and catalytic reaction. An ensemble effect is assumed for the role of alkali hydroxide addition to Rh catalysts used to produce methanol.[5] Besides, the promoting effect may also be due to chemical bifunctional promotion when is catalyzed by Cu.[6] Alkali oxides can neutralize the surface acidic sites of steam reforming catalysts, thus enhancing their resistance to poisoning via acid-catalyzed carbonaceous species from polymerization of the CH_x groups.[7,8,2] In addition to this, many studies suggest that the alkali metal atoms modify the local electron density of the transition metal either directly[9−11] or through the support.[12] However, the chemical state of additives, which are generally introduced as oxides, hydroxides, carbonates, and nitrates, is not well-known.[13,14] Thus, Ertl et al.[10] found that K strongly segregates at the surface, forming a submonolayer of adsorbed K and O having a stoichiometric ratio of unity.

Moreover, alkali addition may result in either a promoting or poisoning effect.[15−16] It has been stated that the addition of 0.3 wt % Na on a $Ni/SiO_2-Al_2O_3$ catalyst increases methanation activity, while with an increase of the sodium content above 2 wt %, the promotion effect is suppressed by some poisoning function of the alkali, either directly via the metal or metal-support interface or via the support itself.[7] In this case, variables such as the nature of the support, the extent of the loading, and the preparation method must be considered. On the other hand, the interaction of alkali moieties with acid carriers affects both the reducibility of supported metal precursors and the dispersity of the metal phase.[16,17] For this reason, the manner in which the support, the metal precursor, and any additive species contact one another helps to define the morphology and size of metal crystallites and the degree of interaction between the metal and other components. In this respect, the distribution of alkali metals on the catalyst surface, especially the nature of the alkali phases present and the amounts on the metal particles and the support, should be elucidated to understand the effects produced by alkali metals on chemisorption properties and catalytic behavior.

In this work, nickel on silica catalysts that are widely used in several industrial processes, such as benzene hydrogenation or fatty oil hydrogenation, was prepared on an alkali-doped silica support. The modified support and the resulting nickel catalysts, with and without the addition of alkali promoters, were comparatively investigated. Nitrogen adsorption measurements, diffuse reflectance IR Fourier transform spectroscopy (DRIFTS) analysis, carbon monoxide-adsorbed DRIFTS studies, quantitative hydrogen chemisorption measurements, X-ray diffraction line broadening (XRDLB), and transmission electron microscopy (CTEM, SAED, and HREM) were used.

Experimental Section

Materials and Treatments. All the samples were prepared by the incipient wetness technique. Undoped Ni/SiO_2 precursor was prepared by adding slowly the required amount of an aqueous solution of $Ni(NO_3)_2 \cdot 6H_2O$ (Merck analytical reagent grade) to the support, silica Kali Chemie AF 125 (100−200 μm size grade), to give a solid with a metallic content of 15 wt %. After impregnation, samples were dried overnight at 393 K and then calcined in an air stream (80 mL/min) for 16 h at 773 K to give the (Si−I) precursor. Three portions of silica were impregnated with aqueous solutions of $LiNO_3$, $NaNO_3$, and KNO_3 (Panreac P.A.), respectively, so that the alkali content reached 1 wt %. These samples were dried and calcined as described above and will be referred to as SiLi, SiNa, and SiK. Alkali-doped catalysts were prepared from these alkali-doped silica samples by means of a second nickel salt impregnation. A $Ni(NO_3)_2 \cdot 6H_2O$ aqueous solution was added to reach a nickel content of 15 wt % and dried and calcined again to give the (SiLi−I), (SiNa−I), and (SiK−I) precursors.

Prior to hydrogen and CO chemisorption measurements, nickel precursor catalysts were reduced in situ at 773 K in a 150 $cm^3\ min^{-1}$ stream of H_2 (heating rate of 8 K min^{-1}) for 14 h. Also, before the reduced samples were exposed to air for X-ray diffraction or electron microscopy measurements, they were passivated at room temperature in an Ar stream (150 $cm^3\ min^{-1}$) containing 100 ppm O_2 for 1.5 h. This treatment is referred to as Rp (e.g., $(Si-I)_{Rp}$).

[†] Present address: Departamento de Química Inorgánica e Instituto de Ciencia de Materiales de Sevilla, Universidad de Sevilla-C.S.I.C., Apdo. 874,41071-Sevilla, Spain.

[‡] On sabbatical leave from Instituto de Física, UNAM A.P. 20-364 01000 México D.F. México.

[§] Departamento de Química Inorgánica e Instituto de Ciencia de Materiales de Sevilla, Universidad de Sevilla-C.S.I.C., Apdo.874,41071-Sevilla, Spain.

* Corresponding author. Phone: (34) 43 216600. Fax: (34) 43 212236.

[⊗] Abstract published in *Advance ACS Abstracts,* February 15, 1997.

S1089-5647(96)03145-8 CCC: $14.00

Nitrogen Adsorption. N_2 adsorption/desorption isotherms of the samples at 77 K were obtained in a Micromeritics ASAP 2000. Samples were previously degassed for 2 h at 473 K and 10^{-3} Torr (1 Torr = 133.3 N m^{-2}). The BET equation was used to calculate the specific surface area, S_{BET}. Total pore volumes, V_p, were estimated at a relative presure of 0.99. The BJH method applied over the desorption isotherm was used to determine the mean pore diameter.

DRIFTS Analysis. DRIFTS spectra were obtained in a Fourier transform Nicolet 5DXC instrument (4000−400 cm^{-1}) in the diffuse reflectance mode. A catalytic chamber (Spectra Tech) with KBr windows allows "in situ" treatments and analysis (room temperature to 875 K). The sample was placed in powdered form in the sample holder and the temperature monitored with a thermocouple located in physical contact with the sample. The resolution was 2 cm^{-1}, and a satisfactory signal-to-noise ratio was obtained by accumulating 200 interferograms. In order to allow comparisons, the silica support was calcined at 773 K prior to DRIFTS measurements.

Spectra of untreated samples were collected at room temperature. Straight away, samples were heated in flowing N_2 at 773 K for 2 h and then were cooled to room temperature, and a spectrum was collected. Samples were subsequently heated at 773 K for 2 h under H_2 flow, and after the reduction treatment, samples were flushed with N_2. The samples were then cooled to room temperature in flowing N_2, and a new spectrum was collected.

Infrared spectroscopy studies of carbon monoxide adsorption were performed after the reduction treatment. A CO stream was diluted with helium (P_{CO} < 5 Torr) (1 Torr = 133.3 N m^{-2}). The spectrum of CO was directly computed from spectra recorded before CO adsorption and after flushing out with excess N_2.

Temperature-Programmed Reduction (TPR). Temperature-programmed experiments were carried out in a conventional flow system (Micromeritics, Pulse Chemisorb 2700) at a heating rate of 10 K/min using a carrier gas flow of 40 mL/min and a thermal conductivity detector. The carrier gas was 19% H_2/N_2, and a cold CO_2/acetone trap was placed between the sample and the detector. The detector response was calibrated by reducing known amounts of CuO.

Hydrogen Chemisorption. H_2 chemisorption data were obtained at room temperature using both the static method in an automatic volumetric apparatus (Micromeritics ASAP 2000C) and the dynamic method with a Micromeritics Pulse Chemisorb 2700. Futher details about the experimentals methods and the expresions used to calculate nickel particle sizes can be found elsewere.[18,19]

Transmission Electron Microscopy (CTEM, SAED, and HREM). Electron microscopy observations were carried out in a Jeol 4000 EX (C_s = 1.00 mm) and a Hitachi 7000 FA. Samples were ground in an agate mortar and then dispersed in isopropyl alcohol in an ultrasonic bath for several minutes. Some drops of this suspension were deposited on a standard copper grid previously covered with a holey carbon film.

X-Ray Diffraction (XRD). XRD patterns were obtained with a Philips APD 1710 powder diffractometer. Nickel-filtered Cu Kα radiation was employed covering 2θ angles between 10° and 85°. The mean crystallite diameters were estimated by application of the Sherrer equation. The width of the Ni-(111) peak at half-maximum was corrected for Kα doublet and instrumental broadening.[20]

Results

Nitrogen Adsorption. The specific surface area (S_{BET}), total pore volume, and BJH mean pore diameter of the samples are reported in Table 1. The total metallic content of each sample, expressed as the number of alkaline, nickel, or total alkaline plus nickel atoms per gram of sample, is also presented in Table 1. It can be seen that alkaline metal impregnation induced an important drop in the silica surface area. Although the total pore volume was not considerably affected, a systematic increase of the mean pore diameter can be observed as the S_{BET} of the sample decreases. Different behavior was found for the nickel-impregnated undoped silica sample. In this case, there was a decrease in the S_{BET}, but the mean pore diameter was not significantly modified. Nevertheless, a decrease in the total pore volume of the sample was observed. Nickel salt impregnation onto the alkali-doped silica produced, with respect to the corresponding alkali-doped support, additional textural changes, arising from a mixture produced by the alkaline impregnation and nickel. These changes were a decrease in S_{BET} and pore volume and an increase in the pore size.

TABLE 1: BET Surface Area (S_{BET}), Total Pore Volume (V_p), BJH Mean Pore Diameter (d_{BJH}) and Metallic Content of the Samples

sample	S_{BET} (m^2 g^{-1})	V_p (cm^3 g^{-1})	d_{BJH} (Å)	metallic content[a] (×10^{-20})
SiO_2	294	0.78	77	
SiLi	149	0.72	134	8.7
SiNa	214	0.73	100	2.6
SiK	236	0.74	92	1.5
(Si−I)	233	0.59	75	15.3
(SiLi−I)	83	0.49	174	24.0
(SiNa−I)	147	0.51	102	17.9
(SiK−I)	138	0.52	110	16.8

[a] Number of alkali, nickel, or total alkali plus nickel atoms per gram of sample.

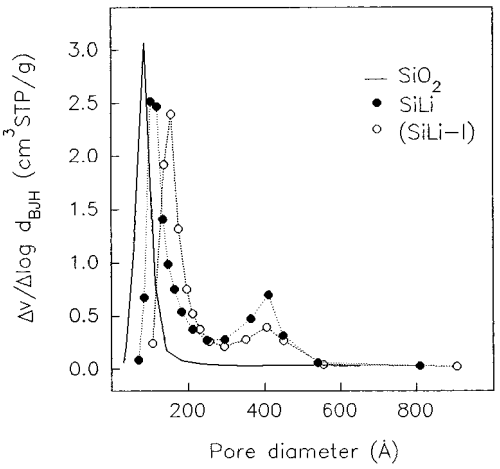

Figure 1. Pore volume distribution for SiO_2, SiLi, and (SiLi−I).

It must be pointed out that, in contrast with the rest of the samples, Li-doped silica and Li-doped nickel catalysts showed a bimodal pore volume distribution. As can be seen in Figure 1, a second maximum of around 400 Å was found in these samples.

Diffuse Reflectance Infrared Spectroscopy (DRIFTS). Spectra of untreated samples under N_2 atmosphere in the 3800−2500 and 2200−1000 cm^{-1} ranges are shown in Figure 2. The 2200−1000 cm^{-1} region has been presented in absorbance units in order to obtain a better representation. In the OH-stretching region, the sharp and intense band at 3749 cm^{-1} ascribed to silica-free hydroxyl groups[21] becomes less intense as the total number of metal atoms impregnated increases. Simoultaneously, the intensity of the broad band between 3700 and 3000 cm^{-1}, ascribed to hydrogen-bonded hydroxyl groups and adsorbed molecular water, also decreased. The main absorption band, peaking at 1360 cm^{-1}, has been ascribed to transverse

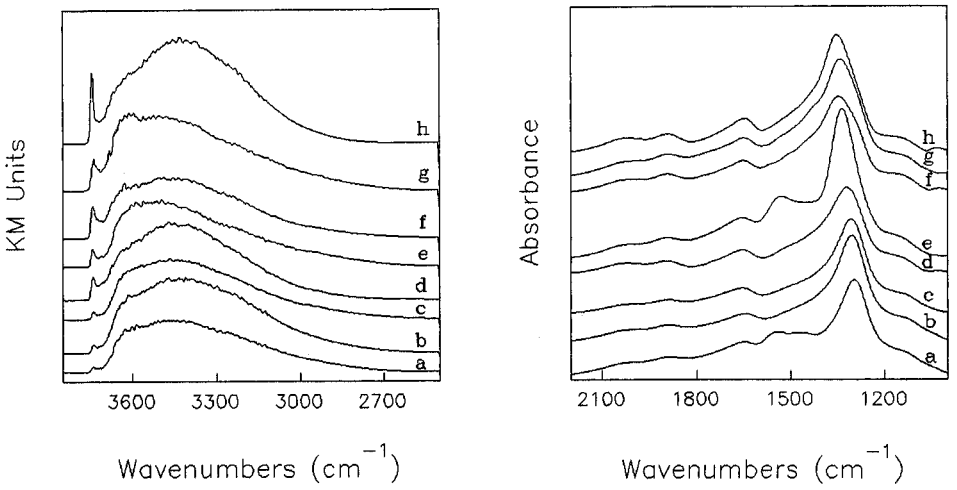

Figure 2. DRIFTS spectra of the untreated samples: (a) (SiLi−I); (b) (SiK−I); (c) (SiNa−I); (d) (Si−I); (e) SiLi; (f) SiK; (g) SiNa; (h) SiO_2.

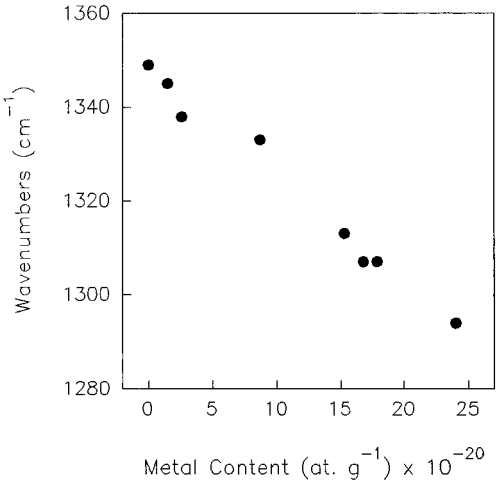

Figure 3. Correlation between the main absorption band of the silica and the metal content of the samples.

(TO) and longitudinal (LO) optical modes of the silica support.[22−23] A linear shift to lower wavenumbers of this band was observed on increasing the metal content of the samples (Figure 3). In addition, new bands at 1530 cm^{-1} in SiLi and at 1550 and 1465 cm^{-1} in (SiLi−I) were observed for the lithium-doped samples. These bands can be ascribed to lithium carbonates.[24]

The spectra after the subsequent reduction treatment are presented in Figure 4. The treatment produced the elimination of adsorbed molecular water (region of 3000−3600 cm^{-1} not shown in Figure 4). The significant decrease of the free

TABLE 2: OH-Stretching Region Integrated Values of DRIFT Spectra

sample	I_N[a]	OH$^-$/nm^2 [b]	I_H[c]	OH$^-_{H2removed}$[d] (%)
SiO_2	61.0	1.8	49.0	20
SiLi	15.0	0.9	11.0	27
SiNa	29.0	1.2	21.0	28
SiK	21.8	0.8	15.0	31
(Si−I)	8.4	0.3	4.0	52
(SiLi−I)	2.4	0.2	0.2	92
(SiNa−I)	3.0	0.2	0.8	73
(SiK−I)	9.0	0.6	0.4	96

[a] Integrated values of samples after heating treatment at 773 K under N_2 atmosphere. [b] Concentration of hydroxyl groups on the surface of samples after heating treatment at 773 K under N_2 atmosphere. [c] Integrated values of samples after reduction treatment. [d] Percentage of hydroxyl groups removed by reduction treatment.

hydroxyl groups on alkali-doped nickel catalysts is clear. Table 2 shows the integrated values for the hydroxyl bands calculated from the spectra resulting from heating the samples at 773 K under N_2 (I_N) and after the reduction treatment (I_H). Assuming, after Zhuravlev,[25] that the hydroxylation degree of silica is independent of its origin and equal to 1.8OH groups per nm^2 for samples outgassed at 773 K, it is possible to estimate the number of hydroxyl groups of the silica support involved in bonding with the added cations (either alkaline or nickel) through the subtraction of hydroxyl coverage on the catalyst or modified support from bare silica (data in Table 2). After the reduction treatment, some extra hydroxyl groups are removed from the samples. This is shown in the last column of Table 2.

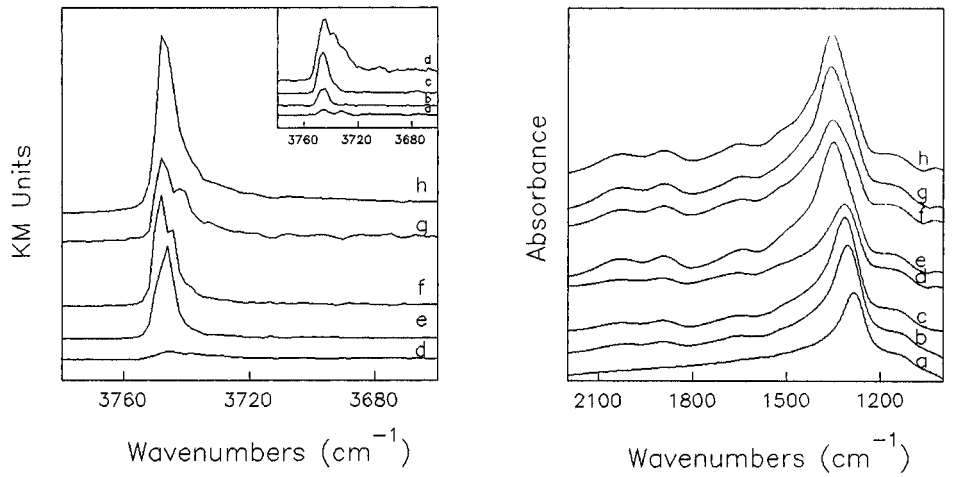

Figure 4. DRIFTS spectra of the reduced samples: (a) (SiLi−I); (b) (SiK−I); (c) (SiNa−I); (d) (Si−I); (e) SiLi; (f) SiK; (g) SiNa; (h) SiO_2.

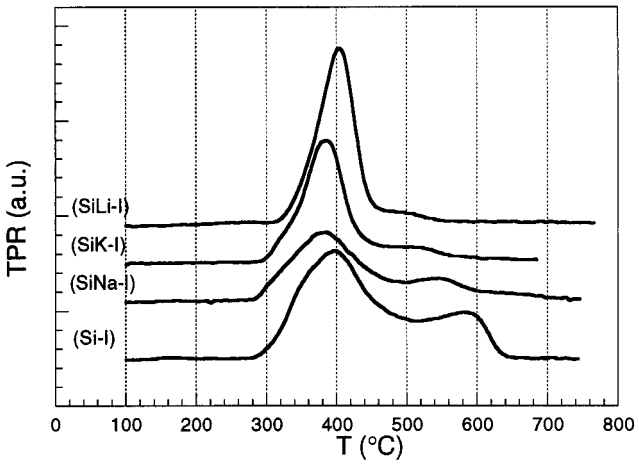

Figure 5. TPR profiles of the samples.

TABLE 3: TPR Maxima Temperatures, Hydrogen Consumption, and Nickel Reduction Degree Calculated from TPR Data

sample	T_{max} T_1 (K)	T_{max} T_2 (K)	H_2 consumption (mmol H_2/g_{cata})	reduction percentage (%)
(Si−I)	652	818	2.71	100
(SiLi−I)	677		3.31	125
(SiNa−I)	656	817	2.95	106
(SiK−I)	658		2.95	101

Temperature-Programmed Reduction (TPR). TPR profiles of the samples are presented in Figure 5. Table 3 presents the temperature of the maxima, the hydrogen consumption, and the corresponding Ni reduction degree. Two peaks were found at 651 and 818 K in the bare (Si−I) catalyst. The same pattern was obtained for the sodium-doped catalyst, although a decrease in the high-temperature area was observed. More evident are the modifications induced in the reduction patterns of the potassium- and lithium-doped catalysts. Single peaks at 658 and 678 K, respectively, were observed in these samples, while the high-temperature peak became a small shoulder. The total hydrogen consumption agrees reasonably well (within 5% error) with the theoretical one calculated for the reduction of NiO to Ni, except for the lithium-doped catalyst (125%).

Hydrogen Chemisorption. Hydrogen uptakes of the bare and alkali-doped nickel catalyst reduced at 773 K are listed in Table 4. For both the static and dynamic methods indicate that potassium and lithium lower the H_2 chemisorption capability of the Ni/SiO_2 system. In all the samples tested, the hydrogen uptake measured by the dynamic method was lower than that measured by the static one and the percentage of reversible hydrogen adsorbed rose in all the alkali-doped catalysts (Table 4). In addition to this, the static/dynamic volume ratio reported in Table 4 varies, with lithium and potassium showing the higher discrepancies between the two methods.

Nickel Particle Size. The estimates of nickel crystallite size from static hydrogen chemisorption, X-ray diffraction line broadening, and transmission electron microscopy are compared in Table 5. The use of the total volume of adsorbed hydrogen is accepted in the literature for particles sizes greater than 1 nm.[26] It must be pointed out that the stoichiometry reported here for total hydrogen adsorption on nickel and determined in a static volumetric system must not be applied to data obtained using flow techniques by means of which irreversible rather than total adsorption is measured. The particle sizes deduced by static H_2 chemisorption were confirmed by XRDLB and TEM, the agreement among the three techniques being in most cases excellent. These results suggest that the decrease in the hydrogen chemisorption uptake for the lithium and potassium nickel catalyst was a consequence of the mean particle increase.

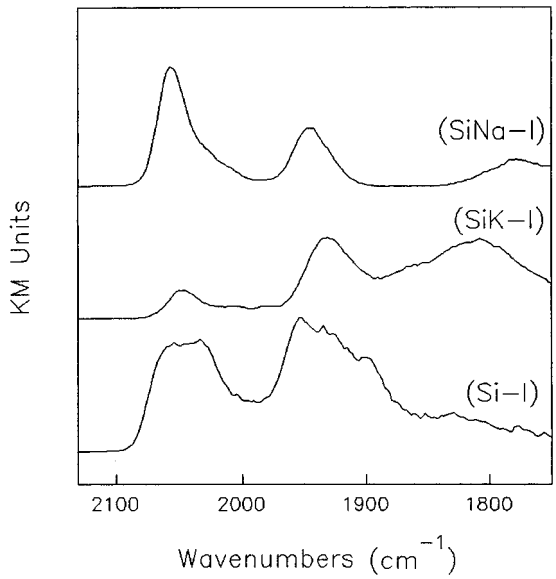

Figure 6. DRIFT spectra of CO irreversibly adsorbed on the reduced samples at 298 K.

TABLE 5: Mean Particle Diameters[a] Obtained by H_2 Chemisorption, XRDLB, and TEM

sample	H_2 chem d_s[b]	XRDLB d_v[c]	TEM d_s[b]	TEM d_v[c]
(Si−I)	9.0	10.2	10.5	11.6
(SiLi−I)	15.6	18.6	15.2	16.7
(SiNa−K)	8.3	8.9	10.2	11.3
(SiK−I)	11.1	12.2	10.8	12.3

[a] Diameters in nm. [b] Surface-averaged values. [c] Volume-averaged values.

Carbon Monoxide Chemisorption. DRIFTS spectra of carbon monoxide adsorbed on catalyst reduced at 773 K, obtained after evacuation of the gas at room temperature, are shown in Figure 6. According to the literature data,[27−30] absorption bands above 2000 cm^{-1} must be ascribed to stretching vibrations of linearly bonded CO, while bands below this frequency are due to bridged and multibonded species. Two peaks centered at 2030 and 2060 cm^{-1} in the linear CO-stretching region and a broad band at 1950 cm^{-1}, probably a combination of two or more unresolved peaks, in the bridge−CO region were found in the bare nickel catalyst. The addition of the alkali induced substantial modifications in the spectrum of the doped catalysts. For the sodium-doped sample, the relative intensity of the band at 2060 cm^{-1}, with respect to the one at 2030 cm^{-1}, increased and the bridge−CO band became a sharper band at 1945 cm^{-1}. Furthermore, a new weak band

TABLE 4: Hydrogen Chemisorption Data

sample	static total (STP cm^3 g^{-1})	static irreversible (STP cm^3 g^{-1})	static reversible (%)	dynamic (STP cm^3 g^{-1})	static/dynamic (ratio)
(Si−I)	2.83	2.09	26.1	1.59	1.78
(SiLi−I)	1.59	0.87	45.3	0.18	8.83
(SiNa−I)	3.17	2.01	36.6	1.64	1.93
(SiK−I)	2.47	1.60	35.2	1.06	2.33

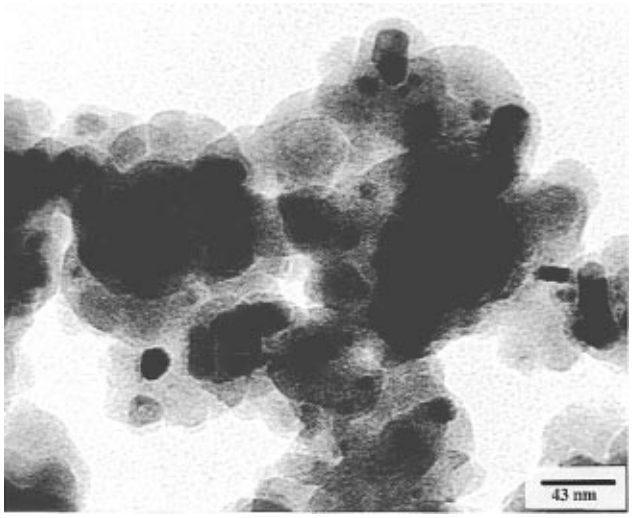

Figure 7. Bright field image of sample $(Si-I)_{Rp}$.The supported metallic phase can be observed presenting different particles sizes.

TABLE 6: Most Probable Phases from SAED and HREM Analysis

	crystalline phases	
sample	SAED	HREM
SiLi	Li_4SiO_4, $LiSiO_2$	
SiNa	NaO_2, NaO_3, Na_2O_2	
SiK	$K_2Si_2O_5$, $K_2Si_4O_9$	
$(SiLi-I)_{R_p}$	$LiSiO_4$, NiO, Ni, Ni_2SiO_4	NiO, Ni_2SiO_4
$(SiNa-I)_{R_p}$	$NaSi_6$, $NaSi_4$, Ni, Na_4SiO_4	NiO, Ni_2SiO_4, Na_4SiO_4
$(SiK-I)_{R_p}$	$K_2Si_4O_9$, K_2NiO_2, Ni	NiO, $Ni_2Si_4O_9$, K_2Si_2O

appeared at 1780 cm^{-1}. The spectrum of the potassium-doped catalyst showed two single peaks at 2050 and 1920 cm^{-1} in the CO linear and bridged regions, respectively. Also, a new low-frequency band was observed at 1800 cm^{-1} for this sample.

Remarkable is the result obtained for the lithium-doped catalyst, where no bands ascribed to carbon monoxide chemisorption on Ni were observed. This result suggested that CO adsorption was strongly inhibited in this sample.

Transmission Electron Microscopy (CTEM, SAED, and HREM). Conventional (CTEM) and high-resolution microscopy (HREM) were performed on the reduced and passivated (Rp) nickel-supported catalysts in order to detect configurations, morphology, distribution of phases, and crystallographic features. Selected area electron diffraction (SAED) methods were applied several times in order to obtain good and readable diffraction patterns over both the alkali-doped supports and the nickel catalysts prepared on them. Only in a few cases were whole and strong reflections obtained because of the characteristics of the samples. The results are presented in Figure 7 and Table 6.

SAED studies performed over the alkali-doped supports allowed mixed phases between silica and the alkaline metal (alkaline silicates) to be detected in the case of K and Li but only alkaline oxides in the case of Na.

CTEM observations of the nondoped nickel catalyst (Figure 7) showed nickel particles (10−20 nm) homogeneously dispersed over the silica support. Similar metallic dispersion (particle sizes) was obtained after impregnation with nickel of the alkali-doped supports (Figures 8a, 9a, and 10a). The distribution of the metallic phase over the support changed in the lithium-doped catalyst, showing a partial aggregation of the nickel particles (Figure 8a).

By SAED and HREM analysis of $(SiLi-I)_{Rp}$, several microcrystalline phases were detected in addition to Ni and NiO, lithium silicate and nickel silicate being the most probable. HREM micrographs showed a close contact between phases, and in some cases, such as in Figure 8c, a relatively big crystallite appeared supporting microcrystallites of a different phase. In sample $(SiNa-I)_{Rp}$, SAED data indicate that, in addition to Ni and NiO, sodium silicides could be present. Nevertheless, the presence of sodium silicide is difficult to accept from a chemical point of view. HREM micrographs also showed a close contact between different phases in this sample. The singular characteristic of the SAED studies on the $(SiK-I)_{Rp}$ sample was that a mixed nickel and potassium silicate could be present in this case. In addition to that, the presence of small clusters of microcrystals of different phases was detected by HREM.

Discussion

Several characterization data suggest important changes in the silica suport due to the presence of the alkaline metals. (i) One is the decrease in surface areas and increase in pore sizes with constant pore volumes. Similar silica-sintering phenomena induced by alkaline metals have been previously reported by Ito et al.[31] and Perrichon et al.[32] The most important textural changes were produced by lithium, which caused even the formation of new pores of about 400 Å. (ii) Another change is formation of alkaline silicates in the case of Li and K but mainly alkaline oxides in the case of Na. (iii) There is a decrease in the silica OH group population proportional to alkaline atom concentrations (Li > Na > K). The TO and LO modes of the silica also shift to lower wavenumbers in proportion to the alkaline content.

From these results, it can be concluded that the interaction between silica and alkaline metals is not just a surface phenomenom but a real structural change. The interaction started on the silica surface (decrease of the OH groups), but during calcination, new phases (observed by SAED and HREM) could be produced, presenting a low melting point and inducing an important dissolution of the support necessary to justify the changes detected in their texture. Differences between samples depend both on the alkaline metal nature and on the atomic concentration.

Impregnation with nickel produced textural changes different from those of alkalis. The decrease in surface area was lower, but in all doped samples the pore volume decreased, the pore size remaining constant. These changes agree with a partial blockage of the porous network without changes in the silica structure.

Finally, after impregnation with nickel of the alkali-doped silica, the modifications observed can be explained by the sum of the two operations but taking into account that the second calcination, after nickel impregnation, also increases the effect of the alkaline metals. In consequence, an additional decrease in surface areas and pore volumes was detected for all the samples. Furthermore, surface OH groups and TO and LO wavenumbers decreased, but even more importantly, new nickel silicate phases in close contact with Ni and NiO and alkaline silicates were detected by SAED and HRTEM.

All these important changes produced by the alkaline dopants must finally result in modifications in the nickel active phase obtained after reduction. These modifications will be discussed in the next three subsections: Reducibility, Nickel Particle Size, and Adsorption Properties.

(i) Reducibility. The TPR pattern obtained for the undoped sample (Si−I) is in agreement with the work of Mile et al.[33,34] Thus, the peaks at 651 and 818 K can be attributed respectively to the reduction of bulk NiO particles and Ni^{++} ions in interaction with the support in the form of a few surface layers of silicate-type compounds. The main difference observed for Li and K samples with respect to the rest of the samples is the

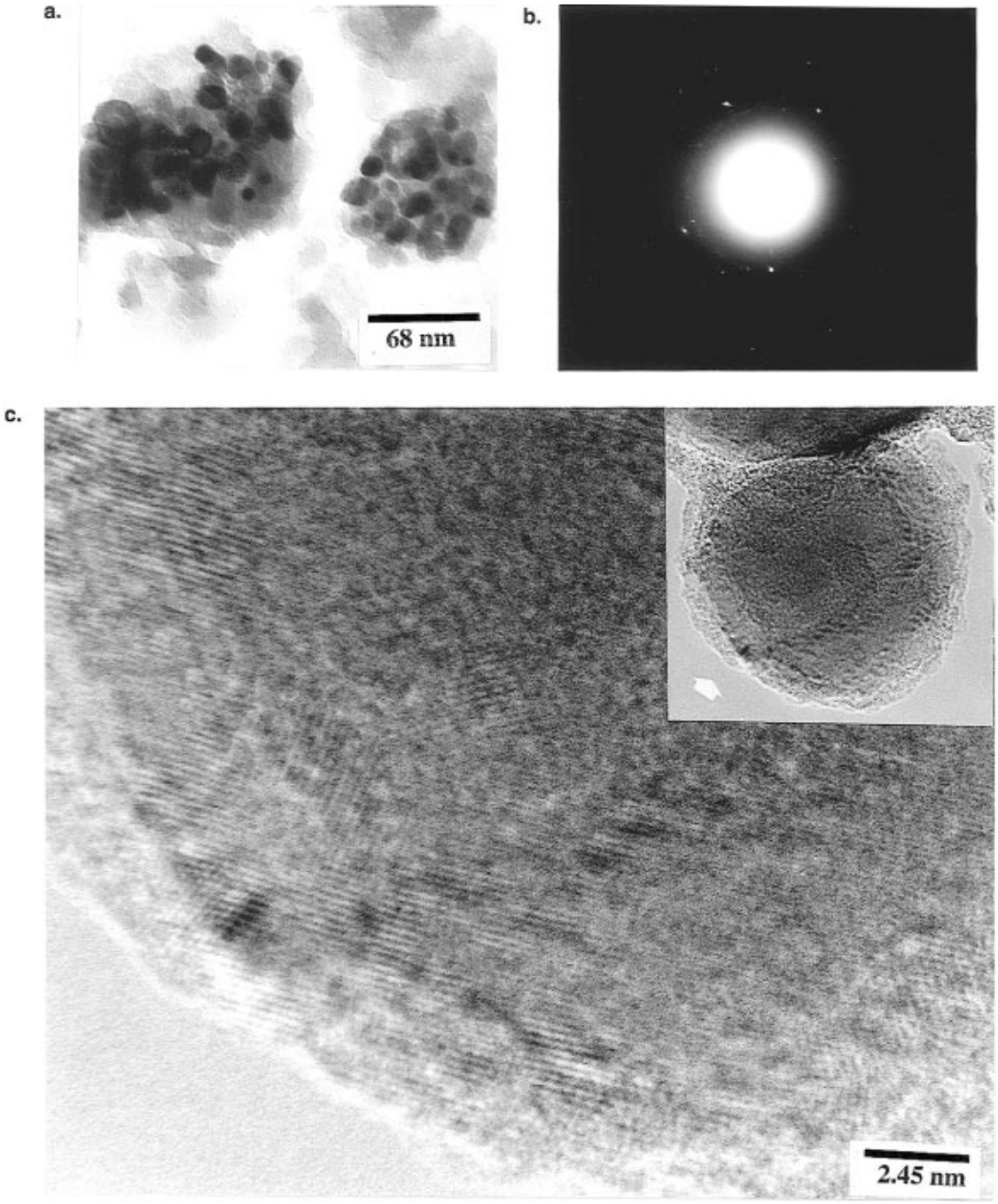

Figure 8. (a) Bright field image of sample $(SiLi-I)_{Rp}$. Agglomerates of metallic particles can be observed. (b) Typical SAED pattern of $(SiLi-I)_{Rp}$ coming from zones similar to the one shown in part a. (c) HREM image of $(SiLi-I)_{Rp}$. In the upper right corner a general view of a big particle with supported crystallites is presented. The zone marked with a white arrow is presented in the magnified image, where lattice spacing coming from different crystalline phases can be observed.

almost complete disappearance of the high-temperature peak corresponding to the nickel interaction compound that, nevertheless, is still present in the Na-doped TPR pattern. This difference could be explained with the SAED and HRTEM data: Li and K formed alkaline silicates, preventing the formation of the nickel silicate, but Na formed sodium oxides, allowing the formation of the nickel−silica interaction compound.

With respect to the hydrogen consumption, the only significant data, showing divergence from the theoretical value corresponding to the reduction NiO → Ni, is the value obtained for the Li-doped sample: 125% reduction degree. When this solid is stored in air at room temperature, the oxide should react to produce hydroxide and carbonate.[35] The presence of carbonate in the precursor was confirned by DRIFTS (bands at 1530−1550 and 1465 cm^{-1} in SiLi and SiLi−I in Figure 2). These bands disappeared after reduction, as confirmed in Figure 4, indicating that part of the hydrogen consumed must be ascribed to the reduction of lithium carbonate. The lithium content of the sample is more than sufficient to justify the additional hydrogen consumption.

(ii) Nickel Particle Size. Nickel particle sizes calculated from hydrogen adsorption data suggest a slight sintering of nickel on the Li- and the K-doped samples, but not present in the case of the Na-doped sample, that presents an even lower particle size. In order to confirm that these results are not artifacts due to changes in the adsorption stoichiometry or saturation coverage, alternative calculations were carried out with CTEM and XRDLB. The results, presented in Table 5, show an excellent ageement between techniques, confirming the different and positive effect of Na on the Ni dispersion. Similar results were reported by Houalla et al.[36] for Na-promoted Ni/SiO_2, explaining

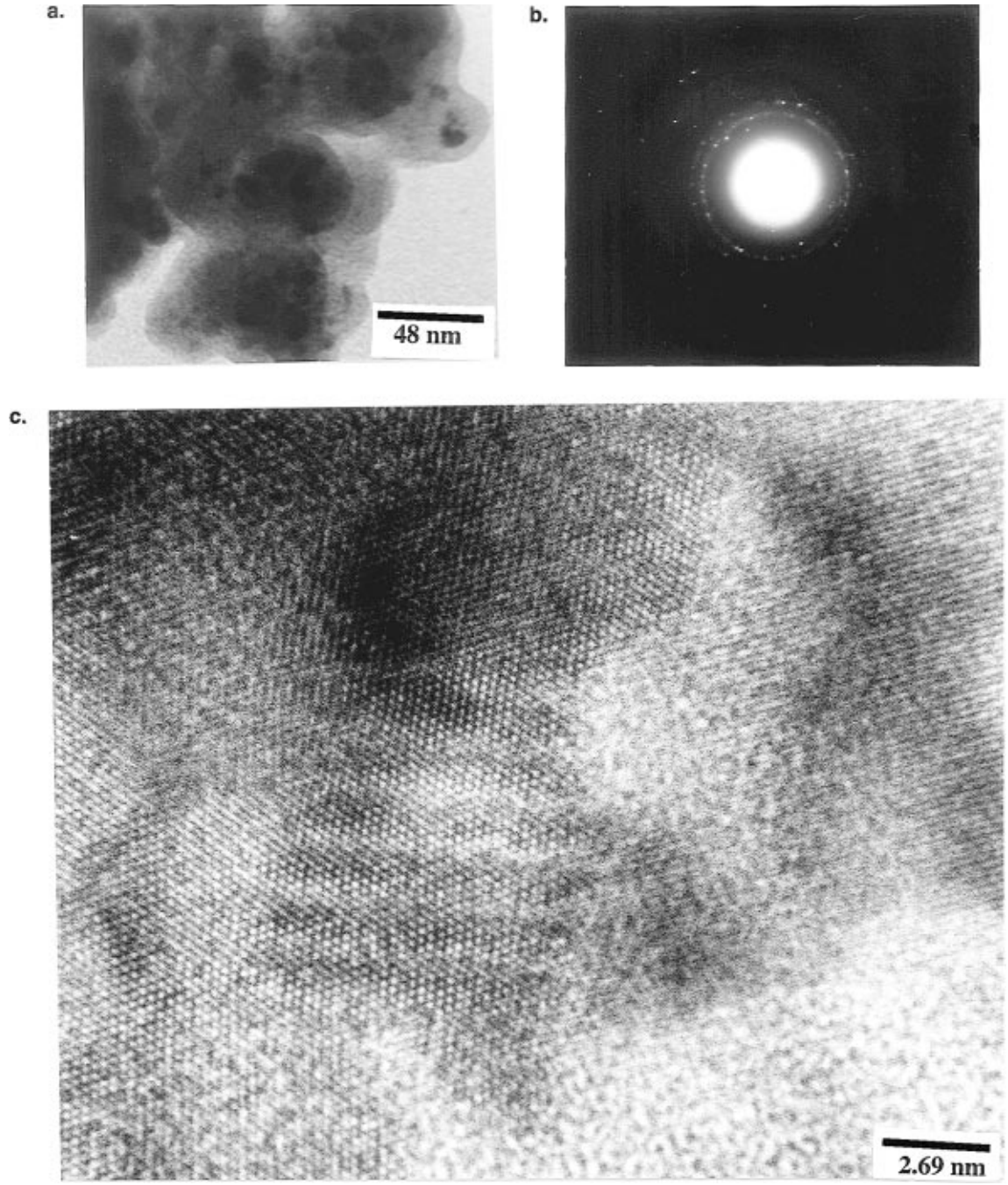

Figure 9. (a) Bright field image of sample $(SiNa-I)_{Rp}$. (b) Typical SAED pattern of $(SiNa-I)_{Rp}$ sample. (c) HREM image from the sample $(SiNa-I)_{Rp}$. The coexistance of two different crystalline phases can be observed.

the nickel dispersion as a result of two opposite effects of Na: The support surface area decrease is counteracted by the barrier action of the Na ions hindering nickel sintering. In our samples, it seems that Li and K compounds are not able to prevent the partial sintering of nickel, which can be expected because of the surface area loss of the support.

(iii) Adsorption Properties. The modification induced by alkali addition on metal adsorption properties has been widely reported in the literature. Kiskinova,[14] studying hydrogen adsorption on alkali-modified nickel found, that these additives give rise to an important decrease in hydrogen dissociation ability and saturation coverage. Other studies on alkali-modified Ni(100) and Ni(111)[37,38] reported that hydrogen adsorption uptake decreases exponentially on increasing alkali coverage. Weatherbee et al.[39] found that potassium produced an increase in the activation energy for hydrogen adsorption on potassium-promoted Fe/SiO_2 catalyst. Thus, Praliaud et al.[40] found that potassium caused a decrease of the hydrogen adsorption and explained this by a decrease in metallic phase accessibility or by a rise of hydrogen bond stoichiometry. Nevertheless, in our work, changes in the total hydrogen adsorption can be explained by the differences produced in the nickel dispersion, as confirmed by CTEM and XRDLB. Thus, no changes in the H−Ni stoichiometry or in the full coverage can be deduced.

However, the reversible fraction of hydrogen uptake in the static method and the static-to-dynamic uptake ratios increased because of the presence of alkaline dopants. Both data suggest that alkaline dopants increase the fraction of the total hydrogen adsorbed in a weak form, in particular with Li.

CO adsorption, evaluated by DRIFTS spectra, showed important changes. It has been reported that CO peaks above 2000 cm^{-1} on supported nickel act as a sensitive probe of the degree of surface smoothness, that is, of the presence of defect sites. The CO region below 2000 cm^{-1} can be a probe for the type of crystal plane exposed if the crystallites are large enough to have extensive smooth planes.[29,30] According to this, the

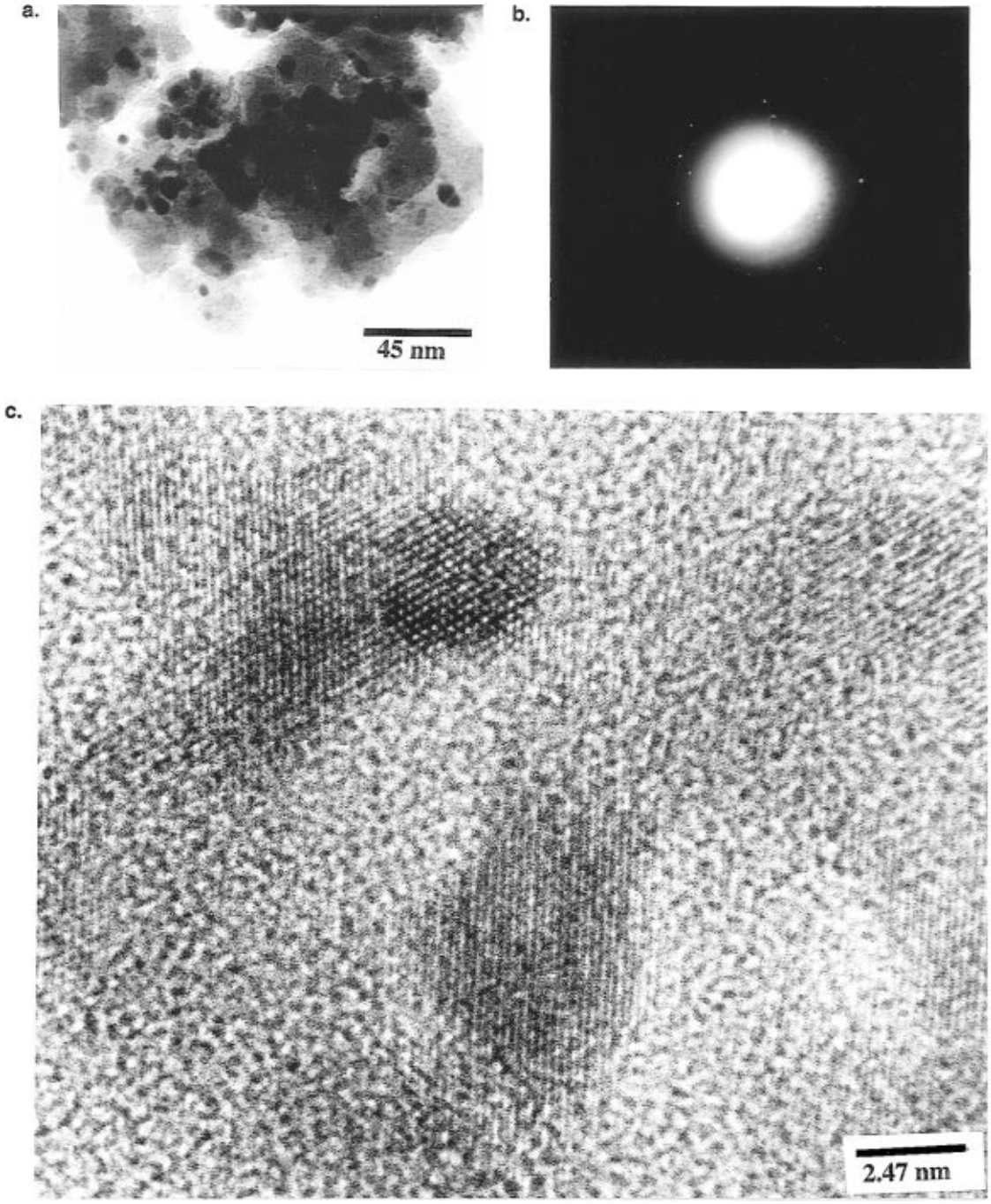

Figure 10. (a) Dispersion of the metallic phase on the support of the $(SiK-I)_{Rp}$ sample. (b) SAED pattern from a zone similar to the one presented in part a. (c) HREM image of $(SiK-I)_{Rp}$ sample. Small particles with different crystallography and different lattice spacings can be observed in this agglomerate similar to that observed in part a.

modification of band shape shown in Figure 6 may suggest changes in the exposed crystal face of Ni particles. On the other hand, several hypotheses have been invoked to explain the low wavenumber band (~1800 cm^{-1}) of adsorbed CO on alkali-promoted metals: (i) face reconstruction, promoting different crystal planes as habitually exposed;[41] (ii) an electron enrichment of the metallic phase, giving rise to an increase in the back donation of the metal electrons to the 2 π^* antibonding CO;[40] (iii) the coordination of the oxygen atom to the alkali cation, which has already been considered for sodium- and potassium-promoted Ni/SiO_2 catalyst.[40,42] A possible localized interaction nickel−carbon monoxide−alkali, with the oxygen atom linked to the alkali cation (oxide, hydroxide, or silicate), located near the metal particles would be in agreement with the presence of an alkali phase at the interphase between the support and nickel at the periphery of the particles reported by Pitchon et al. (43). In our case, HREM observations showing Na- and K-containing phases in close contact with nickel support this hypothesis. In addition to this, face reconstruction induced by interaction with the modified support may be envisaged.

The total CO adsorption inhibition of the lithium-doped catalyst suggests that the surface is blocked for CO adsorption. Because the formation of a $Li_2O/LiOH/Li_2CO$ system has been suggested, and taking into account that LiOH melts at 673 K,[35] it may be reasonable that Li^+ ions, interacting with the forming NiO lattice during air calcination, give rise to the formation of a surface Li−Ni−O mixed phase. In this respect, lithium exhibits some affinity for the NiO lattices. Thus, Li^+ and NiO form $Li_xNi_{(1-x)}O$ solid solution over a wide range ($0 < x < 0.6$) of atomic compositions.[44,45]

In addition to this, the partial dissolution of the support induced by the interaction of alkali moieties with the silica may induce the alteration of the nickel surface in the form of a

"decoration" of the nickel crystallites by alkali species as has been reported in the literature.[2,46]

SAED and HREM data support the formation of a mixed phase K_2NiO_2, in addition to alkali silicates in close contact with the nickel metal particles, as detailed in Figure 7.

However, the fact that a portion of surface Ni sites masked by the Li adlayer phase are inaccessible to CO molecules would appear in contradiction to the hydrogen uptake observed in this sample. In this respect, Praliaud et al.[40,47] pointed out such a phenomenon on a K-doped Ni/SiO_2 catalyst, claiming the occurrence of an alkali-induced "sieving effect", which limits the accessibility of the metal surface to larger probe molecules. Also, Arena et al.[48] observed a decrease in the CO/H_2 adsorption ratio on increasing lithium loading for a Li-doped Ni/MgO catalyst. The good agreement of the mean nickel particle size found between hydrogen chemisorption and XRDLB and TEM suggests that hydrogen is not subject to any hindrance.

It has been shown in Table 2 that H_2 may interact with the modified silica support, removing hydroxyl groups, which would suggest H_2 chemisorption on the support. This is strongly enhanced by the presence of metallic nickel, which results in the removal of up to 96% of the remaining OH groups. On this basis, a radical spillover hydrogen species that interacted with the surface hydroxyl groups[49] could be postulated, being more effective across the basic $Li_2O/LiOH/Li_2CO_3$ medium.[50] Therefore, the high removal of hydroxyls by reaction with spillover hydogen observed on the alkali-doped nickel catalyst may be possible.

Conclusions

Alkali addition yields significant modifications in the physicochemical properties of the Ni/SiO_2 catalyst. The experimental results reported in this study with various alkali metals may be summarized as follows.

(i) Lithium and potasium show a higher reactivity toward the silica, giving rise to alkali silicates that modify the "distribution" of Ni across the support. Lithium, in particular, strongly affects the morphology of the SiO_2, inducing significant sintering of the support. SAED and HREM support the formation of alkali−nickel mixed phases in addition to alkali silicates. Moreover, a close contact between both types of phases and the nickel metal particles has been observed.

(ii) Sodium is mainly present as oxide on the Na-doped silica support. This lesser reactivity toward the silica permits a higher nickel silica interaction and hence the maintenance of nickel particle dispersion with respect to the undoped nickel catalyst.

(iii) The presence of alkaline compounds decorating the Ni particles produced a sieving effect in the adsorption properties. Alkaline dopants induced an increase in the weakly adsorbed fraction of hydrogen and dramatic changes in the adsorption modes of CO, the CO adsorption capacity disappearing completely in the case of the Li-doped sample.

Acknowledgment. We express our thanks to A. Sánchez for nitrogen adsorption measurements and M. Pauli for TPR measurements. The financial support by the Diputación Foral de Gipuzkoa is gratefully appreciated. The support by DGAPA (from UNAM, México) and by the Basque Gouvernment to D.R.A. is also appreciated.

References and Notes

(1) Anderson, R. B. In *Catalysis*; Emmett, P., Ed.; Rheinhold: New York, 1956; Vol. VI.
(2) Mross, W. D. *Catal. Rev. Sci. Eng.* **1983**, *25*, 591.
(3) Chen, I. W.; Shine, D. W. *Ind. Eng. Chem. Res.* **1988**, *27*, 1391.
(4) Chen, I. W.; Chen, F. L. *Ind. Eng. Chem. Res.* **1990**, *29*, 534.
(5) van der Lee, G.; Schuller, B.; Favre, T. L. F.; Post, H.; Ponec, V. *J. Catal.* **1986**, *98*, 522.
(6) van Santen, R. A. *Surf. Sci.* **1991**, *251/252*, 6.
(7) Huang, C. P.; Richardson, J. T. *J. Catal.* **1978**, *51*, 1.
(8) Rostrup-Nielsen, J. R. *Steam Reforming Catalyst*; Danish Technical Press: Copenhagen, 1975; p 81.
(9) Kiskinova, M. P. *J. Surf. Sci.* **1981**, *111*, 584.
(10) Ertl, G.; Weiss, M.; Lee, S. B. *Chem. Phys. Lett.* **1979**, *60*, 391.
(11) Goodman, D. W.; Kiskinova, M. *Surf. Sci.* **1981**, *105*, L265.
(12) Ailka, K.; Hori, H.; Ozaki, A. *J. Catal.* **1972**, *27*, 424.
(13) Ozaki, A.; Aika, K.; Morikawa, Y. In Proceedings, 5th International Congress on Catalysis, Miami Beach, FL, 1972; Hightower, J. W., Ed.; North-Holland: Amsterdam, 1973; p 1251.
(14) Kiskinova, M. P. In *Poisoning and Promotion in Catalysis Based on Surface Science Concepts and Experiments. Studies in Surface Science and Catalysis*; Elsevier: Amsterdam, 1992; Vol. 70, p 149.
(15) Houalla, M.; Delannay, F.; Delmon, B. *J. Phys. Chem.* **1981**, *85*, 1704.
(16) Narayanan, S.; Uma, K. *J. Chem. Soc., Faraday Trans. 1* **1987**, *83*, 733.
(17) Houalla, M.; Lemaitre, J.; Delmon, B. *J. Chem. Soc., Faraday Trans. 1* **1982**, *78*, 1389.
(18) Aguinaga, A.; Montes, M.; de la Cal, J. C.; Asua, J. M. *Ind. Eng. Chem. Res.* **1992**, *31*, 155.
(19) Gandía, L. M. Díaz, A.; Montes, M. *J. Catal.* **1995**, *157*, 461.
(20) Klug, H. P.; Alexander, L. E. *X-Ray Diffraction Procedures*; Wiley: New York, 1974; p 618.
(21) Iler, R. K. *The Chemistry of Silica*; John Wiley & Sons: New York, 1978.
(22) Scott, J. R.; Porto, S. P. *Phys. Rev.* **1967**, *161*, 903.
(23) Benzinger, J. B.; McGoven, S. G.; Royce, B. S. H. In *Catalyst Characterization Science; Surface and Solid State Chemistry*; Deviney, M. L., Gland, J. L., Eds.; ACS Symposium Series 288, The American Society: Washington, DC, 1985; p 449.
(24) Farmer, V. C. In *The Infrared Spectra of Minerals*; Mineralogical Society: London, 1974.
(25) Zhuravlev, L. T. *Langmuir* **1987**, *3*, 316.
(26) Anderson, J. R.; Pratt, K. C. In *Introduction to Characterization and Testing of Catalyst*; Academic Press: Sydney, Australia, 1985.
(27) Primet, M.; Dalmon, J. A.; Martin, G. A. *J. Catal.* **1977**, *46*, 25.
(28) Rochester, C. H.; Terrell, R. J. *J. Chem. Soc., Faraday Trans. 1* **1977**, *73*, 609.
(29) Blackmond, D. B.; Ko, E. I. *J. Catal.* **1985**, *96*, 210.
(30) Sheppard, N.; Nguyen, T. T. In *Advances in Infrared and Raman Spectroscopy*; Clarke, P. J., Hester, R. E., Eds.; Wiley: New York, 1978; Vol. 5, p 67.
(31) Ito, T.; Wang, J. X.; Lin, C. H.; Lunsford, J. H. *J. Am. Chem. Soc.* **1985**, *107*, 5062.
(32) Perrichon, V.; Durupty, M. C. *Appl. Catal.* **1988**, *42*, 217.
(33) Mile, B.; Stirling, D.; Zammitt, M.; Lovell, A.; Webb, M. *J. Catal.* **1988**, *114*, 217.
(34) Mile, B.; Stirling, D.; Zammitt, M.; Lovell, A.; Webb, M. *J Mol. Catal.* **1988**, *62*, 179.
(35) Andersen, A. G.; Norby, T. *Catal. Today* **1990**, *6*, 575.
(36) Houalla, M.; Delannay, F.; Delmon, B. *Preprints of the 7th Canadiam Symposium on Catalysis*; Wanke, S. E., Chakrabarty, S. K., Eds.; Chemical Institute of Canada: Edmonton, 1980; p 158.
(37) Sun, Y. M.; Luftman, H. S.; White, J. M. *Surf. Sci.* **1984**, *139*, 379.
(38) Lanzilloto, A. M.; Dresser, M. J.; Alvey, M. D.; Yates, J. T. *J. Chem. Phys.* **1988**, *89*, 570.
(39) Weatherbee, G. D.; Rankin, J. L.; Bartholomew, C. H. *Appl. Catal.* **1984**, *11*, 73.
(40) Praliaud, H.; Primet, M.; Martin, G. A. *Appl. Surf. Sci.* **1983**, *17*, 107.
(41) Deliagianni, H.; Mieville, R. L.; Peri, J. B. *J. Catal.* **1985**, *95*, 465.
(42) Uram, K. J.; Ng, L., Jr.; Yates, J. T. *Surf. Sci.* **1986**, *177*, 253.
(43) Pitchon, V.; Gallezot, P.; Nicot, C.; Praliaud, H. *Appl. Catal.* **1989**, *47*, 357.
(44) Bielanski, A.; Deren, J.; Haber, J.; Sloczynski, J. *Trans. Faraday Soc.* **1966**, *58*, 166.
(45) Marini, A.; Berbenni, V.; Massarotti, V.; Flor, G.; Riccardi, R.; Leonini, M. *Solid State Ionics* **1989**, *32/33*, 398.
(46) Praliaud, H.; Dalmon, J. A.; Microdatos, C.; Martin, G. A. *J. Catal.* **1986**, *97*, 344.
(47) Martin, G. A.; Praliaud, H. *Catal. Lett.* **1991**, *9*, 151.
(48) Arena, F.; Chuvilin, A. L.; Parmaliana, A. *J. Phys. Chem.* **1995**, *99*, 990.
(49) Conner, W. C.; Falconer, J. L. *Chem. Rev.* **1995**, *95*, 759.
(50) Dalmon, J. A.; Mirodatos, C.; Turlier, P.; Martin, G. A. In *Studies in Surface Science Catalysis. Spillover of Adsorbed Species*; Pajonk, G. M., Teichner, S. J., German, J. E., Eds.; Elsevier: Amsterdam, The Netherlands, 1982; Vol. 17, p 169.